Geometrical Formulation of 3D Space-Time Finite Integration Method

Jun Kawahara, Takeshi Mifune, and Tetsuji Matsuo, *Member, IEEE*

Graduate School of Engineering, Kyoto University, Kyoto 615-8510, Japan

A geometrical formulation of a space-time finite integration (FI) method is studied for application to electromagnetic wave propagation calculations. Based on the Hodge duality and Lorentzian metric, a modified relation is derived between the incidence matrices of space-time primal and dual grids. A systematic method to construct the Maxwell grid equations on the space-time primal and dual grids is developed. The geometrical formulation is implemented on a simple space-time grid, which is proven equivalent to an explicit time-marching scheme of the space-time FI method.

***Index Terms*—Finite integration method, graph theory, Hodge duality, space-time grid.**

I. Introduction

THE finite integration (FI) method [1]-[5] has been studied to accomplish time-domain electromagnetic field computations using unstructured spatial grids. The FI method derives grid-based Maxwell equations using incidence matrices based on the dual computational-grid geometry. Graph theory enables a systematic construction of the spatial dual grid from the primal grid geometry. However, the geometry description is restricted to the spatial domain. Accordingly, similar to the FDTD method [6], the FI method uses a uniform time-step, which is restricted by the Courant-Friedrichs-Lewy condition [7] based on the smallest spatial grid size.

Previous work [8] introduced a space-time FI method that achieves non-uniform time-steps naturally on the three- dimensional (3D) space-time grid with 2D space. The Hodge dual grid was proposed in [9] to construct the 4D space-time grid for electromagnetic field computation. An application of space-time FI method to a photonic band computation was reported in [12]. However, it is not always a simple task to construct the Maxwell grid equations on these dual space-time grids. To realize a systematic derivation of Maxwell grid equations, a graph-theory-based formulation for the space-time dual grids is required. This paper discusses a geometrical formulation of the 3D space-time FI method that is based on the Hodge duality and the Lorentzian metric but is not a straightforward extension of the conventional spatial FI formulation.

II. Finite Integration Method on a Space-Time Grid

A. Electromagnetics in Space-Time

The Maxwell equations are described in the differential form as

$$\mathrm{d}F = 0, \quad \mathrm{d}G = J. \tag{1}$$

Manuscript received October 31, 2012; revised December 27, 2012 (date on which paper was submitted for review). Corresponding author: T. Matsuo (email: tmatsuo@kuee.kyoto-u.ac.jp).

Digital Object Identifier inserted by IEEE

In the coordinate system $(x^0, x^1, x^2, x^3) = (t, x, y, z), F, G$ and J are written as

$$\begin{aligned} F &= -\Sigma_{i=1}^3 E_i \mathrm{d}x^0 \mathrm{d}x^i + \Sigma_{j=1}^3 B_j \mathrm{d}x^k \mathrm{d}x^l, \\ G &= \Sigma_{i=1}^3 H_i \mathrm{d}x^0 \mathrm{d}x^i + \Sigma_{j=1}^3 D_j \mathrm{d}x^k \mathrm{d}x^l, \\ J &= c\rho \mathrm{d}x^1 \mathrm{d}x^2 \mathrm{d}x^3 - \Sigma_{j=1}^3 cJ_j \mathrm{d}x^0 \mathrm{d}x^k \mathrm{d}x^l \end{aligned} \tag{2}$$

where c is the speed of light, ρ is the electric charge density and (j, k, l) is a cyclic permutation of $(1, 2, 3)$. The integral form of (1) is given as

$$\oint_{\partial\Omega_\mathrm{p}} F = 0, \quad \oint_{\partial\Omega_\mathrm{d}} G = \int_{\Omega_\mathrm{d}} J \tag{3}$$

where Ω_p and Ω_d are hypersurfaces in space-time.

For simplicity, assuming the uniformity along the z-direction, this paper discusses the FI formulation for the electromagnetic field (B_z, E_x, E_y) in the (w, x, y)-3D free space-time [8], where $w = ct$. Accordingly, F and G are written as

$$\begin{aligned} F &= B_z \mathrm{d}x\mathrm{d}y + \mathcal{E}_y \mathrm{d}y\mathrm{d}w - \mathcal{E}_x \mathrm{d}w\mathrm{d}x, \\ G &= \mathcal{H}_z \mathrm{d}w - D_y \mathrm{d}x + D_x \mathrm{d}y \end{aligned} \tag{4}$$

where $(\mathcal{E}_x, \mathcal{E}_y) = (E_x/c, E_y/c)$, $\mathcal{H}_z = H_z/c$. Defining 3D vectors $\boldsymbol{F}$ and $\boldsymbol{G}$ as

$$\boldsymbol{F} = (B_z, \mathcal{E}_y, -\mathcal{E}_x), \quad \boldsymbol{G} = (\mathcal{H}_z, -D_y, D_x) \tag{5}$$

the integral form is written without source term as

$$\oint_S \boldsymbol{F} \cdot \boldsymbol{n} \mathrm{d}S = 0, \quad \oint_C \boldsymbol{G} \cdot \boldsymbol{t} \mathrm{d}s = 0 \tag{6}$$

where $\boldsymbol{n}$ is the normal vector at each point on the closed surface S and $\boldsymbol{t}$ the tangent vector at each point on the closed curve C. The Euclidean metric is used for the dot product operation.

The space-time FI method uses discretized variables as

$$f = \int_p \boldsymbol{F} \cdot \boldsymbol{n} \mathrm{d}S, \quad g = \int_{\tilde{s}} \boldsymbol{G} \cdot \boldsymbol{t} \mathrm{d}s \tag{7}$$

where p is a face of a primal grid and $\tilde{s}$ is an edge of a dual grid. To express the constitutive equation between f and g simply, $\boldsymbol{n}$ and $\boldsymbol{t}$ are given as [8]

$$\boldsymbol{n} = (n_w, n_x, n_y), \quad \boldsymbol{t} = (n_w, -n_x, -n_y). \tag{8}$$

Fig. 1 illustrates the geometrical relation between $\boldsymbol{n}$ and $\boldsymbol{t}$, where $\tilde{s}$ is orthogonal to p in the Lorentzian 3D space-time. The relation between $\boldsymbol{F} \cdot \boldsymbol{n}$ and $\boldsymbol{G} \cdot \boldsymbol{t}$ is given as

$$\boldsymbol{F} \cdot \boldsymbol{n} = Z\boldsymbol{G} \cdot \boldsymbol{t} \tag{9}$$

where Z is the impedance of the medium. Thus, f is related to g as

$$f = zg \tag{10}$$

$$z = Z\frac{\Delta S}{\Delta l} \tag{11}$$

where ΔS is the area of p and Δl is the length of $\tilde{s}$.

Ref. [9] extended the dual-grid construction above to the 4D space-time, called the Hodge dual grid. It is based on the Hodge duality with the Lorentzian metric between F and G, where the metric is modified in materials depending on the speed of light.

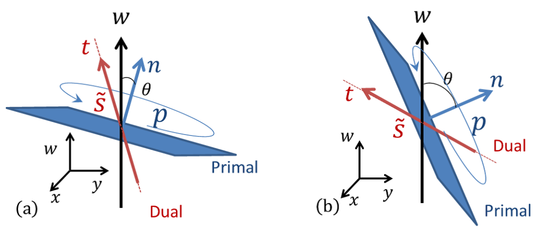

Fig. 1: Relation of primal face and dual edge in space-time grid when (a) $\boldsymbol{n} \cdot \boldsymbol{t} > 0$ and (b) $\boldsymbol{n} \cdot \boldsymbol{t} < 0$.

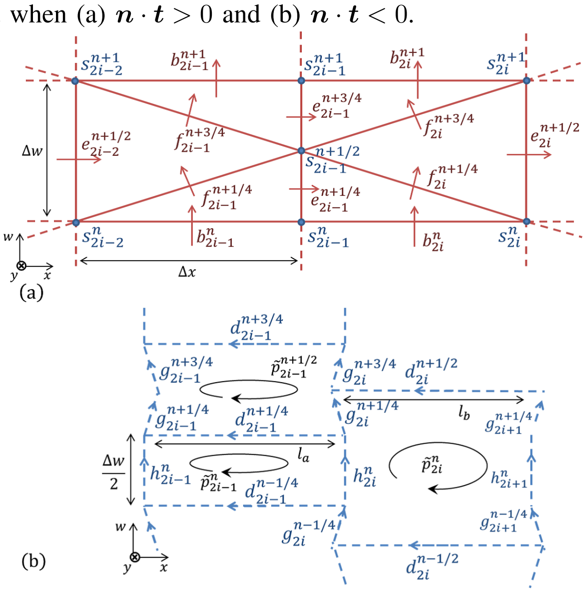

Fig. 2: Edges and faces on (a) the primal grid and (b) the dual grid.

B. Explicit Time-Marching Scheme

Refs. [8] and [9] have shown explicit time-marching schemes for 3D and 4D space-time FI analyses of electromagnetic wave propagation. This subsection presents an explicit time-marching scheme on a simple 2D space-time grid with 1D space to relate to the geometrical formulation described later.

Fig. 2 illustrates 2D space-time primal and dual grids that have temporal step sizes Δw and $\Delta w/2$ and spatial step size Δx along the x- and y- directions.

Based on (5) and (7), the variables in Fig. 2 have the following meaning; b: magnetic flux, e: electromotive force, f: the composition of b and e, h: magnetomotive force, d: electric flux, and g: the composition of h and d. The arrow directions in Fig. 2 are based on (7) and (9) using the definition (5) and (8). Note that the arrow direction of d is opposite to that of e. These do not correspond directly to the directions of $\boldsymbol{E}$ and $\boldsymbol{D}$ in the Euclidean space.

The explicit time-marching scheme is given as follows. According to a numerical examination in [10], the scheme is stable when $(l_a - 1)^2 + (\Delta w)^2/2 < 1$.

Variables $d_{2i-1}^{n+1/4}$ and $e_{2i-1}^{n+1/4}$ are given as

$$d_{2i-1}^{n+1/4} = d_{2i-1}^{n-1/4} - (h_{2i}^n - h_{2i-1}^n) \tag{12}$$

$$e_{2i-1}^{n+1/4} = z_{e1} d_{2i-1}^{n+1/4}, \quad z_{e1} = Z\frac{\Delta w \Delta x}{2l_a}. \tag{13}$$

On the primal grid, $f_{2i-1}^{n+1/4}$, $f_{2i}^{n+1/4}$ and consequently $g_{2i-1}^{n+1/4}$, $g_{2i}^{n+1/4}$ are given as

$$\begin{aligned} f_{2i-1}^{n+1/4} &= -e_{2i-1}^{n+1/4} + b_{2i-1}^n, \\ f_{2i}^{n+1/4} &= e_{2i-1}^{n+1/4} + b_{2i}^n \end{aligned} \tag{14}$$

$$g_k^{n+1/4} = \frac{1}{z_f} f_k^{n+1/4} (k = 2i-1, 2i), \; z_f = Z\frac{4\Delta x^2}{\Delta w}. \tag{15}$$

On the dual grid, d_{2i} and e_{2i} are updated using

$$\begin{aligned} d_{2i}^{n+1/2} &= d_{2i}^{n-1/2} + h_{2i}^n - h_{2i+1}^n \\ &\quad + g_{2i}^{n-1/4} - g_{2i+1}^{n-1/4} + g_{2i}^{n+1/4} - g_{2i+1}^{n+1/4} \end{aligned} \tag{16}$$

$$e_{2i}^{n+1/2} = z_{e2} d_{2i}^{n+1/2}, \; z_{e2} = Z\frac{\Delta w \Delta x}{2 - l_a + (\Delta w)^2/4}. \tag{17}$$

Similarly, $f_{2i-1}^{n+3/4}$, $f_{2i}^{n+3/4}$ and $g_{2i-1}^{n+3/4}$, $g_{2i}^{n+3/4}$ are given as

$$\begin{aligned} f_{2i-1}^{n+3/4} &= f_{2i-1}^{n+1/4} + e_{2i-2}^{n+1/2}, \\ f_{2i}^{n+3/4} &= f_{2i}^{n+1/4} - e_{2i}^{n+1/2} \end{aligned} \tag{18}$$

$$g_k^{n+3/4} = \frac{1}{z_f} f_k^{n+3/4} (k = 2i-1, 2i). \tag{19}$$

On the dual grid, $d_{2i-1}^{n+3/4}$ and $e_{2i-1}^{n+3/4}$ are obtained from

$$\begin{aligned} d_{2i-1}^{n+3/4} &= d_{2i-1}^{n+1/4} + g_{2i-1}^{n+1/4} - g_{2i}^{n+1/4} \\ &\quad + g_{2i-1}^{n+3/4} - g_{2i}^{n+3/4} \end{aligned} \tag{20}$$

$$e_{2i-1}^{n+3/4} = z_{e1} d_{2i-1}^{n+3/4}. \tag{21}$$

Hence, b_{2i-1}^{n+1}, b_{2i}^{n+1} and h_{2i-1}^{n+1}, h_{2i}^{n+1} are given by

$$\begin{aligned} b_{2i-1}^{n+1} &= f_{2i-1}^{n+3/4} - e_{2i-1}^{n+3/4}, \\ b_{2i}^{n+1} &= f_{2i}^{n+3/4} + e_{2i-1}^{n+3/4} \end{aligned} \tag{22}$$

$$h_k^n = \frac{1}{z_b} b_k^n \, (k = 2i-1, 2i), \quad z_b = Z\frac{2\Delta x^2}{\Delta w}. \tag{23}$$

C. Incidence Matrices on 3D Euclidean Space

The FI method is generally formulated with the Maxwell grid equations using the incidence matrices from graph theory.

Let arrays $\{n\}$, $\{s\}$, $\{p\}$ and $\{v\}$ denote the sets of nodes, edges, faces, and volumes in the primal grid, respectively. These are related by incidence matrices $[G]$, $[C]$ and $[D]$ [1], [2], [11] as

$$\partial\{s\} = [G]\{n\},\ \partial\{p\} = [C]\{s\},\ \partial\{v\} = [D]\{p\} \tag{24}$$

where ∂ denotes restriction to the boundary. Similarly, the sets of nodes, edges, faces and volumes in the dual grid are related as

$$\partial\{\tilde{s}\} = [\tilde{G}]\{\tilde{n}\},\ \partial\{\tilde{p}\} = [\tilde{C}]\{\tilde{s}\},\ \partial\{\tilde{v}\} = [\tilde{D}]\{\tilde{p}\}. \tag{25}$$

In the Euclidean space, the dual grid is generally constructed so the incidence matrices satisfy

$$[\tilde{C}] = [C]^{\mathrm{T}},\ [\tilde{D}] = -[G]^{\mathrm{T}},\ [\tilde{G}] = -[D]^{\mathrm{T}}. \tag{26}$$

The relation above derives the Maxwell grid equations systematically from the primal grid geometry.

The space-time primal and dual grids based on (8) have a similar property to that described by (26), which gives the one-to-one correspondence between the faces $\{p\}$ on the primal grid and the edges $\{\tilde{s}\}$ on the dual grid. However, the directional relation between $\{p\}$ and $\{\tilde{s}\}$ determined by (8) differs from that given by (26). The following subsection derives the matrix relation for the space-time primal and dual grids based on (8).

D. Incidence Matrices on 3D Space-Time

A simple space-time primal grid illustrated in Fig. 3 is examined. Assuming spatial periodicity in the grid geometry, the edges s_i and faces p_i are periodically numbered for notational simplicity. Moreover, the edges and faces perpendicular to the y-axis is omitted. The direction of edges s_1, s_2, s_3, s_1', s_2' is along the $+y$-direction. The edge $\tilde{s}_i$ on the dual grid corresponds to the face p_i on the primal grid, where their directions satisfy (8).

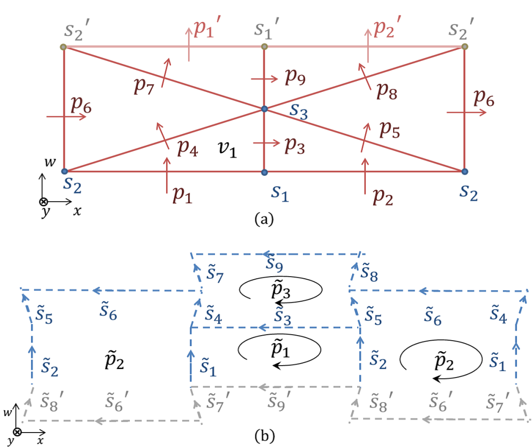

Fig. 3: Edges and faces on (a) the primal grid and (b) the dual grid.

The geometrical relation between edges and faces on the primal grid is represented by the following equations.

$$\begin{aligned}&\partial p_1 = s_1 - s_2,\ \partial p_2 = -s_1 + s_2,\ \partial p_3 = s_1 - s_3,\\ &\partial p_4 = -s_2 + s_3,\ \partial p_5 = s_2 - s_3,\ \partial p_6 = s_2 - s_2',\\ &\partial p_7 = s_3 - s_2',\ \partial p_8 = -s_3 + s_2',\ \partial p_9 = s_3 - s_1'.\end{aligned} \tag{27}$$

To examine the relation between $[C]$ and $[\tilde{C}]$, a subset of $\{s\}$ and a subset of $\{p\}$ are defined as

$$\{s\}_{\mathrm{sb}} = [s_1 \quad s_2 \quad s_3]^{\mathrm{T}},\ \{p\}_{\mathrm{sb}} = [p_1 \quad p_2 \ \cdots \ p_9]^{\mathrm{T}}. \tag{28}$$

Omitting s_1', s_2', relation (27) is written $\{p\}_{\mathrm{sb}} = [C]_{\mathrm{sb}}\{s\}_{\mathrm{sb}}$ where $[C]_{\mathrm{sb}}$ is a submatrix of $[C]$ and given as

$$[C]_{\mathrm{sb}}^{\mathrm{T}} = \begin{bmatrix} 1 & -1 & 1 & 0 & 0 & 0 & 0 & 0 & 0 \\ -1 & 1 & 0 & -1 & 1 & 1 & 0 & 0 & 0 \\ 0 & 0 & -1 & 1 & -1 & 0 & 1 & -1 & 1 \end{bmatrix}. \tag{29}$$

On the dual grid, the relation between edges and faces is found to be:

$$\begin{aligned}&\partial\tilde{p}_1 = \tilde{s}_1 - \tilde{s}_2 - \tilde{s}_3 + \tilde{s}_9',\\ &\partial\tilde{p}_2 = -\tilde{s}_1 + \tilde{s}_2 - \tilde{s}_4 + \tilde{s}_5 - \tilde{s}_6 + \tilde{s}_6' - \tilde{s}_7' + \tilde{s}_8',\\ &\partial\tilde{p}_3 = \tilde{s}_3 + \tilde{s}_4 - \tilde{s}_5 + \tilde{s}_7 - \tilde{s}_8 - \tilde{s}_9.\end{aligned} \tag{30}$$

Corresponding to $\{s\}_{\mathrm{sb}}$ and $\{p\}_{\mathrm{sb}}$, subsets of $\{\tilde{p}\}$ and $\{\tilde{s}\}$ are defined as

$$\{\tilde{p}\}_{\mathrm{sb}} = [\tilde{p}_1 \quad \tilde{p}_2 \quad \tilde{p}_3]^{\mathrm{T}},\ \{\tilde{s}\}_{\mathrm{sb}} = [\tilde{s}_1 \quad \tilde{s}_2 \cdots \tilde{s}_9]^{\mathrm{T}}. \tag{31}$$

Omitting $\tilde{s}_6'$, $\tilde{s}_7'$, $\tilde{s}_8'$, $\tilde{s}_9'$, relation (30) is written as $\{\tilde{p}\}_{\mathrm{sb}} = \{\mathrm{C}\}_{\mathrm{sb}}\{\tilde{s}\}_{\mathrm{sb}}$ where $\{\tilde{C}\}_{\mathrm{sb}}$ is a submatrix of $[\tilde{C}]$ and given as

$$[\tilde{C}]_{\mathrm{sb}} = \begin{bmatrix} 1 & -1 & -1 & 0 & 0 & 0 & 0 & 0 & 0 \\ -1 & 1 & 0 & -1 & 1 & -1 & 0 & 0 & 0 \\ 0 & 0 & 1 & 1 & -1 & 0 & 1 & -1 & -1 \end{bmatrix}. \tag{32}$$

Comparing $[\tilde{C}]_{\mathrm{sb}}$ with $[C]_{\mathrm{sb}}^{\mathrm{T}}$ shows that the elements of $[\tilde{C}]_{\mathrm{sb}}$ at the 3rd, 6th, and 9th columns have opposite signs to the corresponding elements of $[C]_{\mathrm{sb}}^{\mathrm{T}}$. This sign inversion caused by (8) is illustrated in Fig. 1. If $\boldsymbol{n}$ and $\boldsymbol{t}$ given by (8) satisfy $\boldsymbol{n}\cdot\boldsymbol{t} < 0$, the direction of the edge is opposite to the direction of the face as depicted in Fig. 1(b).

Consequently, the incidence matrix $[\tilde{C}]$ of dual grid based on (8) is given as

$$[\tilde{C}] = [C]^{*\mathrm{T}} \tag{33}$$

where the operator $*\mathrm{T}$ is determined by the mapping

$$\tilde{c}_{ij} = \begin{cases} c_{ji}, & (c_{ji} \neq 0 \ \text{and} \ \boldsymbol{n}\cdot\boldsymbol{t} > 0) \\ -c_{ji}, & (c_{ji} \neq 0 \ \text{and} \ \boldsymbol{n}\cdot\boldsymbol{t} < 0) \\ 0, & (c_{ji} = 0) \end{cases}. \tag{34}$$

This relation is a consequence of the Hodge duality between $\boldsymbol{F}$ and $\boldsymbol{G}$ based on the Lorentzian metric in the 3D space-time. Using $\boldsymbol{n}\cdot\boldsymbol{t} = n_w^2 - n_x^2 - n_y^2$, the matrix $[C]^{*\mathrm{T}}$ can be obtained without the need for the dual grid.

Using $[\tilde{C}]$, the electromagnetic field equations on the dual grid such as (12), (16) and (20) are expressed as

$$[\tilde{C}]\{g\} = 0 \tag{35}$$

where $\{g\}$ consists of the variables defined by the second equation of (7) on the edges corresponding to $\{\tilde{s}\}$.

The relation between faces and volumes on the primal grid is represented similarly. For instance, the volume surrounded by p_1, p_3, and p_4 is written:

$$\partial v_1 = -p_1 + p_3 + p_4. \tag{36}$$

These relations are represented by matrix $[D]$ in the form given by the third equation of (24). Using $[D]$, the electromagnetic field equations on the primal grid such as (14), (18) and (22) are expressed as

$$[D]\{f\} = 0. \tag{37}$$

where $\{f\}$ consists of the variables defined by the first equation of (7) on the faces corresponding to $\{p\}$.

Fig. 4 summarizes the geometric relation above. In the 3D Euclidean space, $\boldsymbol{E}$ and $\boldsymbol{B}$ are assigned separately to the edges and faces, respectively whereas these are unified into $\boldsymbol{F}$ and assigned to the faces in the 3D space-time.

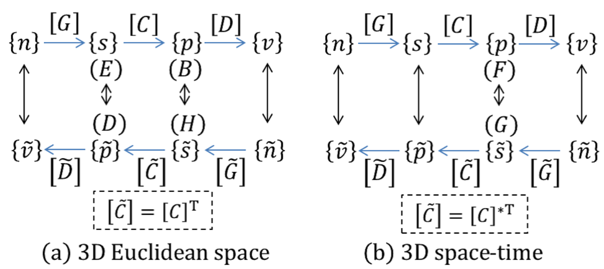

Fig. 4: Duality and matrix relations.

E. Maxwell Grid Equations

From (10), $\{g\}$ is related to $\{f\}$ as

$$\{f\} = [z]\{g\} \tag{38}$$

where $[z]$ is a diagonal matrix of which elements are given by (11).

Equations (33), (35), (37), and (38) derive the space-time Maxwell grid equations systematically

$$\begin{bmatrix} [D] \\ [C]^{*\mathrm{T}}[z]^{-1} \end{bmatrix} \{f\} = 0. \tag{39}$$

By modifying the impedance matrix, another formulation is possible, where relation $[\tilde{C}] = [C]^{\mathrm{T}}$ holds. The modified impedance matrix $[z^*]$ is defined by replacing the elements of $[z]$ by $-Z\Delta S/\Delta l$ when $\boldsymbol{n} \cdot \boldsymbol{t} < 0$. Thereby, $[C]^{*\mathrm{T}}[z]^{-1} = [C]^T[z^*]^{-1}$ holds.

F. Application Example in 2D Space-Time Grid

The FI method formulated by (39) is implemented and compared with the FI scheme explained in Subsection II.B. The propagation of an electromagnetic wave with components (E_y, B_z) is computed on the periodic 2D space-time grid shown in Fig. 2 with $\Delta x = 1, i = 1, \cdots, 50$, $\Delta w = 0.5, n = 0, \cdots, 80$, and $l_a = 1$. The initial condition at $w = 0$ is given as $B_z = \exp(-x^2/25)$ and $E_y = 0$. The impedance matrix $[z]$ consists of z_{e1}, z_{e2}, z_f, and z_b that are given as (13), (15), (17) and (23). The spatially periodic boundary condition is imposed where $e_0^n = e_{80}^n$ and $h_{81}^n = h_1^n$.

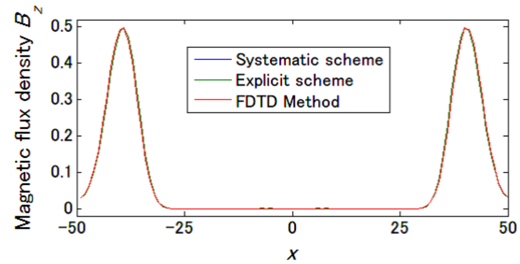

Fig. 5: Magnetic flux distribution at $w = 40$.

Fig. 5 shows the distribution of B_z at $w = 80\Delta w$, where the simulation result given by the FDTD method is also shown for comparison. The FI formulation (39) is equivalent to the FI scheme given in II.B.

III. Concluding Remarks

A geometrical formulation of the 3D space-time FI method was presented that provides a systematic method to construct the Maxwell grid equations on the space-time primal and dual grids. The relation between the incidence matrices of these space-time grids was derived based on the Hodge duality with Lorentzian metric.

Practically, the systematic formulation is used to derive or confirm the explicit time-marching scheme. The extension to the 4D space-time and its practical application will be addressed in the near future.

References

[1] T. Weiland, "Time domain electromagnetic field computation with finite difference methods," *Int. J. Numer. Model.*, vol. 9, pp. 295-319, 1996.

[2] A. Bossavit and L. Kettunen, "Yee-like schemes on a tetrahedral mesh, with diagonal lumping," *Int. J. Numer. Model*. vol. 12, pp. 129-142, 1999.

[3] I. E. Lager, E. Tonti, A.T. de Hoop, G. Mur, and M. Marrone, "Finite formulation and domain-integrated field relations in electromagnetics - a synthesis," *IEEE Trans. Magn.*, vol. 39, pp. 1199-1202, May 2003.

[4] P. Alotto, A. De Cian, and G. Molinari, "A time-domain 3-D full-Maxwell solver based on the cell method," *IEEE Trans. Magn.*, vol. 44, pp. 799-802, Apr. 2006.

[5] L. Codecasa and M. Politi, "Explicit, consistent, and conditionally stable extension of FD-TD to tetrahedral grids by FIT," *IEEE Trans. Magn.*, vol. 44, pp. 1258-1261, June 2008.

[6] K. S. Yee, "Numerical solution of initial boundary value problems involving Maxwell's equations in isotropic media," *IEEE Trans. Antennas Propagat.*, vol. 14, pp. 302-307, May 1966.

[7] A. Talfove and S. C. Hagness, *Computational Electromagnetics, The Finite Difference in Time Domain Method*, 3rd Ed., Artech House, Boston, 2005.

[8] T. Matsuo, "Electromagnetic field computation using space-time grid and finite integration method," *IEEE Trans. Magn.*, vol. 46, pp. 3241-3244, Aug. 2010.

[9] T. Matsuo, "Space-time finite integration method for electromagnetic field computation," *IEEE Trans. Magn.*, vol. 47, pp. 1530-1533, Apr. 2011.

[10] S. Shimizu, T. Mifune, and, T. Matsuo, "Space-time grids for electromagnetic field computation using finite integration method," APS-URSI Spokane, pp. 2346 - 2349, 2011.

[11] A. Bossavit, *Computational Electromagnetism*, Academic Press, 1998.

[12] T. Shimoi, T. Mifune, T. Matsuo, and Y. Tanaka, "Finite integration method using local fine grid for explicit electromagnetic field computation," in Digests 15th CEFC Oita, TP2-4, p. 201, 2012.